

Electron states and magnetic phase diagrams of strongly correlated systems

V. Yu. Irkhin¹ and P. A. Igoshev^{1,2}

¹*M. N. Mikheev Institute of Metal Physics, 620108 Ekaterinburg, Russia and*

²*Ural Federal University, 620002 Ekaterinburg, Russia*

Various auxiliary-particle approaches to treat electron correlations in many-electron models are analyzed. Applications to copper-oxide layered systems are discussed. The ground-state magnetic phase diagrams are considered within the Hubbard and *s-d* exchange (Kondo) models for square and simple cubic lattices vs. band filling and interaction parameter. A generalized Hartree-Fock approximation is employed to treat commensurate ferro-, antiferromagnetic, and incommensurate (spiral) magnetic phases, and also magnetic phase separation. The correlations are taken into account within the Hubbard model by using the slave-boson approach. The main advantage of this approach is correct estimating the contribution of doubly occupied states number and therefore the paramagnetic phase energy.

PACS numbers: 71.27.+a, 75.10.Lp, 71.30.+h

Magnetic properties of strongly correlated transition-metal compounds and their relation to doping, lattice geometry, band structure and interaction parameters are still being extensively investigated. In particular, the details of magnetic order in the ground state remain to be examined both theoretically and experimentally. During recent decades, the two-dimensional (2D) case closely related to the problem of high-temperature superconductivity in cuprates and iron arsenides has been intensively investigated theoretically.

The ground state of strongly correlated systems is characterized by a competition of ferromagnetic (FM) and antiferromagnetic (AFM) ordering which results in occurrence of spiral magnetic ordering [1] or the magnetic phase separation [1–3]. The consideration of these problems is performed within a number of many-electron models. In the present work we discuss theoretical approaches to treat these model within auxiliary-particle representations (Sect.1) and present some results of numerical calculations (Sect.2).

I. THEORETICAL MODELS AND SLAVE PARTICLE REPRESENTATIONS

To describe the properties of such systems one uses many-electron models like the Hubbard, *s-d* exchange (Kondo) and Anderson lattice models. These are widely applied, *e. g.*, for high- T_c cuprates and rare earth compounds. There exist some relations (mappings) between these models in various parameter regions.

The Hamiltonian of the Hubbard model reads

$$\mathcal{H}_H = \sum_{ij\sigma} t_{ij} c_{i\sigma}^\dagger c_{j\sigma} + U \sum_i n_{i\uparrow} n_{i\downarrow}, \quad (1)$$

where $c_{i\sigma}^\dagger$ are electron creation operators. In the limit of large Hubbard parameter U and band filling $n < 1$ (hole doping) this is reduced to the $t - J$ model

$$\mathcal{H}_{t,J} = - \sum_{ij\sigma} t_{ij} X_i(0\sigma) X_j(\sigma 0) + \sum_{ij} J_{ij} \mathbf{S}_i \mathbf{S}_j. \quad (2)$$

where $X_i(\Gamma, \Gamma') = |\Gamma_i\rangle \langle \Gamma'_i|$ are the Hubbard X-operators acting on the i site local subspace [4], $J_{ij} = 2t_{ij}^2/U$.

To proceed with analytical and numerical calculations, it is convenient to use auxiliary (“slave”) boson and fermion representations. In connection with the theory of high-temperature superconductors, Anderson [5] put forward the idea of the separation of the spin and charge degrees of freedom of electron ($\sigma = \pm 1$):

$$c_{i\sigma}^\dagger = X_i(\sigma, 0) + \sigma X_i(2, -\sigma) \rightarrow f_{i\sigma}^\dagger e_i + \sigma d_i^\dagger f_{i-\sigma}. \quad (3)$$

Here, $f_{i\sigma}^\dagger$ are the creation operators for neutral fermions (spinons), and e_i^\dagger , d_i^\dagger are the creation operators for charged spinless bosons (holons and doublons). For large U , we have to retain only holon or doublon degrees of freedom for hole or electron doping, respectively.

In fact, the choice of the Fermi statistics for spinons and Bose one for holons is not unique and can be varied depending on the physical picture (*e.g.*, presence or absence of magnetic ordering, see also [6]). Thus, the spin operators in Eq. (2) are presented as the bilinear form

$$\mathbf{S}_i = \frac{1}{2} \sum_{\sigma\sigma'} a_{i\sigma}^\dagger \boldsymbol{\sigma}_{\sigma\sigma'} a_{i\sigma'}, \quad (4)$$

in terms of Schwinger bosons ($a_{i\sigma}^\dagger = b_{i\sigma}^\dagger$) or fermionic spinons ($a_{i\sigma}^\dagger = f_{i\sigma}^\dagger$), $\boldsymbol{\sigma}$ being Pauli matrices.

A more complicated representation proposed by Kotliar and Ruckenstein [7] introduces the slave boson operators e_i , $p_{i\sigma}$, d_i , so that

$$c_{i\sigma}^\dagger \rightarrow f_{i\sigma}^\dagger z_{i\sigma}^\dagger \quad (5)$$

where $f_{i\sigma}$, $f_{i\sigma}^\dagger$ are the slave Fermi operators, and

$$z_{i\sigma}^\dagger = (1 - e_i^\dagger e_i - p_{i-\sigma}^\dagger p_{i-\sigma})^{-1/2} (p_{i\sigma}^\dagger e_i + d_i^\dagger p_{i-\sigma}) \times (1 - d_i^\dagger d_i - p_{i\sigma}^\dagger p_{i\sigma})^{-1/2}. \quad (6)$$

There exists also a rotationally invariant version [11]

$$c_{i\sigma}^\dagger = \sum_{\sigma'} f_{i\sigma}^\dagger z_{i\sigma\sigma'}^\dagger, \quad \hat{z}_i = e_i^\dagger \hat{L}_i M_i \hat{R}_i \hat{p}_i + \hat{p}_i^\dagger \hat{L}_i M_i \hat{R}_i d_i \quad (7)$$

where the factors L, M, R are similar to those in (6), the scalar and vector slave boson fields p_{i0} and \mathbf{p}_i are introduced as $\hat{p}_i = \frac{1}{2}(p_{i0}\sigma_0 + \mathbf{p}_i\boldsymbol{\sigma})$ and $\hat{\tilde{p}}_i$ is the time reverse of operator \hat{p}_i . This version is suitable for magnetically ordered phases to take into account spin fluctuation corrections. In particular, it can describe in a simple way non-quasiparticle states owing electron-magnon scattering which were earlier treated in the many-electron representation of Hubbard's operators (cf. Ref.[8]).

We mention also the rotor representation [9]

$$c_{i\sigma}^\dagger = f_{i\sigma}^\dagger \exp(i\theta_i) \quad (8)$$

where the original Hubbard interaction is replaced in by a simple kinetic term for the phase field, $(U/2)\hat{L}_i^2$, with the angular momentum $\hat{L} = -i\partial/\partial\theta$. This representation is suitable to describe the metal-insulator transition in the paramagnetic phase.

In the case of the Anderson lattice model transport and magnetic properties are separated between different systems, s and d correspondingly:

$$\begin{aligned} \mathcal{H}_A = & \sum_{ij\sigma} t_{ij} c_{i\sigma}^\dagger c_{j\sigma} + \epsilon_d \sum_{i\sigma} d_{i\sigma}^\dagger d_{i\sigma} \\ & + V \sum_{i\sigma} (c_{i\sigma}^\dagger d_{i\sigma} + d_{i\sigma}^\dagger c_{i\sigma}) + U \sum_i d_{i\uparrow}^\dagger d_{i\uparrow} d_{i\downarrow}^\dagger d_{i\downarrow}, \end{aligned} \quad (9)$$

ϵ_d is the energy of localized (' d -electron') state, V is on-site s - d hybridization providing the coupling between these subsystems.

Provided that the d -level is well below the Fermi energy and Coulomb interaction is sufficiently large ($|V| \ll \epsilon_F - \epsilon_d, U$), this model can be reduced by the Schrieffer-Wolff transformation to the s - d exchange model

$$\mathcal{H}_{s-d} = \sum_{\mathbf{k}\sigma} t_{\mathbf{k}} c_{\mathbf{k}\sigma}^\dagger c_{\mathbf{k}\sigma} - I \sum_{i\sigma\sigma'} (\mathbf{S}_i \cdot \boldsymbol{\sigma}_{\sigma\sigma'}) c_{i\sigma}^\dagger c_{i\sigma'}, \quad (10)$$

with spin $S = 1/2$ and the exchange parameter

$$I = V^2 [1/(\epsilon_d - \epsilon_F) - 1/(U + \epsilon_d - \epsilon_F)], \quad (11)$$

where ϵ_F is the Fermi level.

Remember also the three-band model of cuprates

$$\begin{aligned} \mathcal{H} = & \sum_{\mathbf{k}a\sigma} \left[\epsilon p_{\mathbf{k}a\sigma}^\dagger p_{\mathbf{k}a\sigma} + \Delta d_{\mathbf{k}\sigma}^\dagger d_{\mathbf{k}\sigma} + V_{\mathbf{k}} (p_{\mathbf{k}\sigma}^\dagger d_{\mathbf{k}\sigma} + h.c.) \right] \\ & + U \sum_i d_{i\uparrow}^\dagger d_{i\uparrow} d_{i\downarrow}^\dagger d_{i\downarrow}, \end{aligned} \quad (12)$$

where ϵ and Δ are positions of p - and d -levels for O- and Cu-ions, $V_{\mathbf{k}} = 2V_{pd} (\sin^2 k_x + \sin^2 k_y)^{1/2}$ are the matrix elements of p - d hybridization (cf. [10]). In the large- U limit we can use the slave boson representation $d_{i\sigma}^\dagger \rightarrow X_i(\sigma_0) = f_{i\sigma}^\dagger e_i$.

For $|V_{pd}| \ll \epsilon - \Delta$ (large charge-transfer gap) the Hamiltonian (12) is again reduced by a canonical transformation to the t - J model with $t_{\text{eff}} = V_{pd}^2/(\epsilon - \Delta)$. It

is interesting that the t - J model obtained from the one-band Hubbard model is also formally reduced to a similar structure in the representation (7) with auxiliary rather than physical particles p_i . Thus the Hubbard model and the model (12) can be considered in a parallel way [10].

To describe doped cuprates, also a representation of the Fermi dopons $d_{i\sigma}^\dagger$ was proposed [13, 14]

$$X_i(0, -\sigma) = -\frac{\sigma}{2\sqrt{2}} \sum_{\sigma'} d_{i\sigma'}^\dagger (1 - n_{i, -\sigma'}) [\delta_{\sigma\sigma'} - 2(\mathbf{S}_i \boldsymbol{\sigma}_{\sigma'\sigma})]. \quad (13)$$

On substituting (13) into the t - J Hamiltonian (2) we obtain the terms which are linear in spin operators. These can provide hybridization between electrons (dopons) and Fermi spinons to describe nodal-antinodal dichotomy and formation of large Fermi surface in cuprates with the increase of doping [14]. Thus the initial one-band model takes the form of an effective two-band model. Note that a similar structure is obtained in the spin-rotation representation (7).

On the other hand, in the antiferromagnetic case it is convenient to use the Schwinger rather than the spinon representation (see (4)). Such an approach was developed in [12] to describe the formation of spin liquid state in terms of frustrations in localized-spin subsystems. The supersymmetry approach [15] mixes the fermionic and the bosonic representation of the spin following the standard rules of superalgebra.

II. RESULTS OF NUMERICAL CALCULATIONS

After the local rotation in the spin space matching the local magnetization vectors at different sites, say along z axis, (which is necessary for the consideration of magnetic spirals) by the angle $\mathbf{Q}\mathbf{R}_i$ (where \mathbf{Q} is the wave vector of the spiral) the Hubbard Hamiltonian in the slave boson representation (6) takes the form

$$\mathcal{H}_{\text{eff}} = \sum_{ij\sigma\sigma'} t_{ij}^{\sigma\sigma'} f_{i\sigma}^\dagger f_{j\sigma'} z_{i\sigma}^\dagger z_{j\sigma'} + U \sum_i d_i^\dagger d_i, \quad (14)$$

with $t_{ij}^{\sigma\sigma'} = \exp[i\mathbf{Q}(\mathbf{R}_i - \mathbf{R}_j)\sigma^x]_{\sigma\sigma'} t_{ij}$. This form enables us to construct the mean-field approximation where the boson averages do not depend on lattice site.

The calculations were performed for the half-filled Hubbard model to describe the metal-insulator transition and for the magnetic phase diagram for arbitrary filling [3, 16, 17]. Here we present the results for the square (Fig. 1) and simple cubic (Fig. 2) lattices in the Hubbard model within the Hartree-Fock approximations (HFA) and slave boson approach (SBA) in the mean-field version and within HFA for the s - d exchange model [3, 18].

One can see that HFA yields the variety of spiral magnetic phases, as well as FM and AFM ones at sufficiently large U generally and at any U in the vicinity of half-filling. The account of correlations (SBA) leads to a

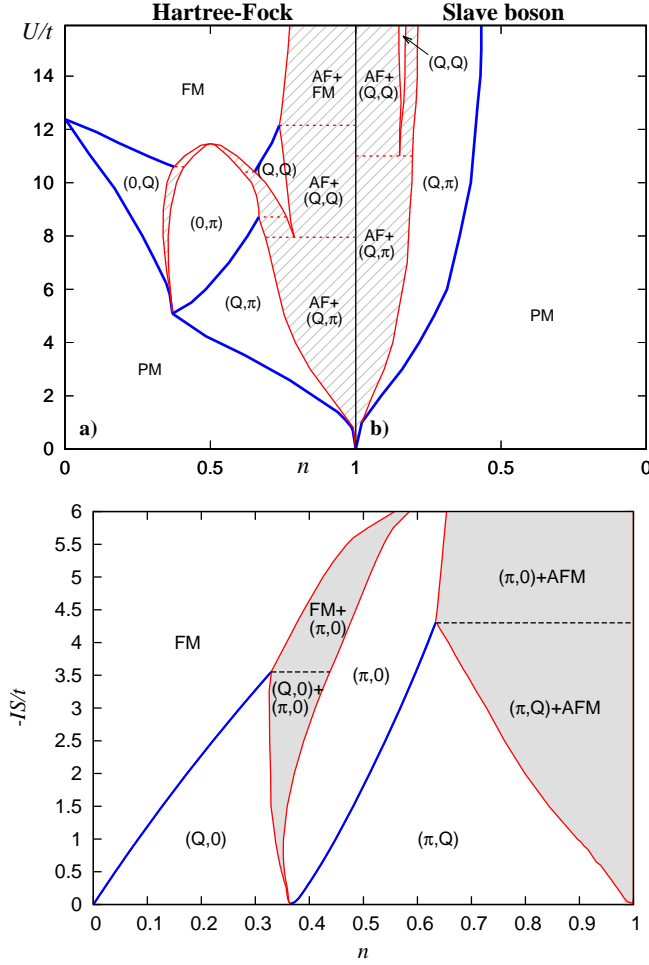


FIG. 1: (Color online) Ground state magnetic phase diagram of the Hubbard model (upper panel, within (a) HFA and (b) SBA) and s - d model (lower panel) for the square lattice at $n < 1$. The spiral phases are denoted according to the form of their wave vector. Filling shows the phase separation regions, dashed (red) lines being the boundaries between different phase pairs. Bold (blue) lines denote the second-order phase transitions. Solid (red) lines correspond to the boundaries between a homogeneous phase and phase separation region, $\mathbf{Q}_{\text{AFM}} = (\pi, \pi)$.

noticeable suppression of magnetically ordered states in comparison with HFA: the corresponding density intervals in the phase diagram decrease strongly, and the variety of the spiral states disappears. Besides that, in SBA there occurs a wide region of paramagnetic (PM) state which is a manifestation of correct treatment of the energy of doubles.

It should be stressed that only SBA provides a correct description of large U case at finite density of current carriers, whereas the ground state energy in HFA is divergent at $U \rightarrow \infty$ due to overestimation of Coulomb interaction energy, as well as in random phase approximation (RPA) [19].

Within the mean-field approximation, the Hubbard model is equivalent to the s - d model with the replace-

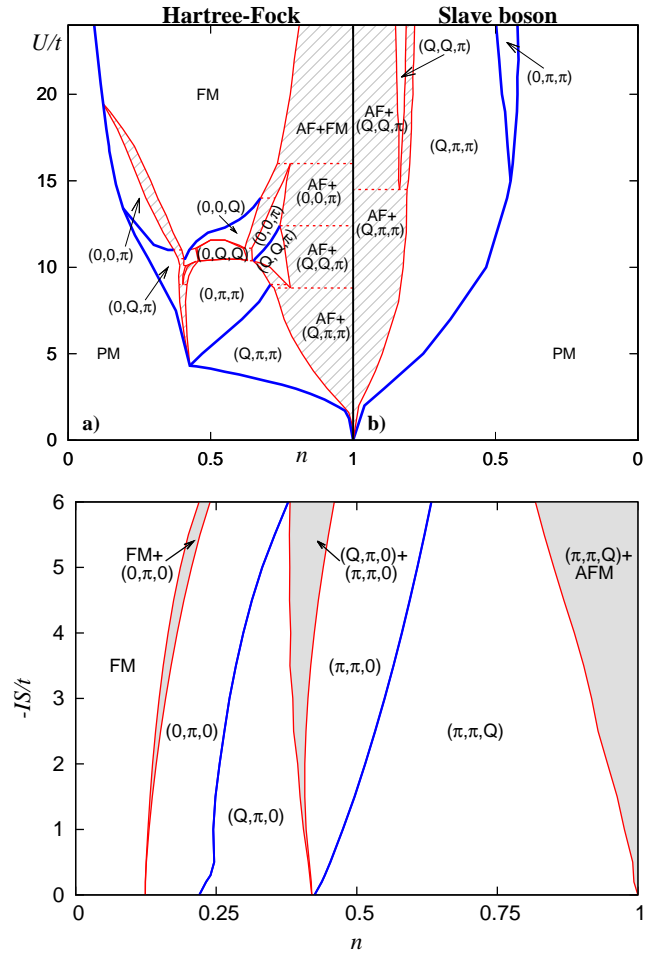


FIG. 2: (Color online) The phase diagrams for the simple cubic lattice. Notations are the same as in Fig. 1, $\mathbf{Q}_{\text{AFM}} = (\pi, \pi, \pi)$.

ment $IS = Um/2$. However, the phase separation condition and description of the PM phase are different in these models. Thus the phases are strongly redistributed.

Due to existence of localized moments, ferromagnetic ordering in the s - d model is favorable already at small $|I|$, whereas within the Hubbard model it occurs at sufficiently large U only. The increase of $|I|$ results in a growth of FM region. At small $|I|$ the wave vector of magnetic phase is specified by the position of the maximum of the Lindhardt function

$$\chi_{\mathbf{Q}}^0 = \frac{1}{N} \sum_{\mathbf{k}} \frac{f_{\mathbf{k}+\mathbf{Q}} - f_{\mathbf{k}}}{t_{\mathbf{k}} - t_{\mathbf{k}+\mathbf{Q}}} \quad (15)$$

calculated in the PM phase ($f_{\mathbf{k}}$ is the Fermi function).

An important difference of the square and simple cubic lattice (2D and 3D) cases is the form of FM region at small n . In the former case its width vanishes at $I \rightarrow 0$, but in the latter case the width is finite and sufficiently large, the transition to the spiral $(0, \pi, 0)$ phase being of the first order. For the square lattice, the spiral phases are fully suppressed by FM and AFM regions at $|IS| \gtrsim$

6*t*. For the simple cubic lattice, the spiral phases turn out to be more stable. For small number of carriers in the AFM matrix ($1 - n \ll 1$), the phase separation between AFM and spiral ((Q, π) for square lattice and (Q, π, π) for simple cubic lattice) phases is present at small interaction parameter.

The research was carried out within the state assignment of FASO of Russia (theme “Quantum” No. AAAA-A18-118020190095-4). This work was supported in part by Ural Division of RAS (project no. 18-2-2-11) and by the Russian Foundation for Basic Research (project no. 16-02-00995).

-
- [1] P.A. Igoshev, M.A. Timirgazin, A.A. Katanin, A.K. Arzhnikov, and V.Yu. Irkhin, Incommensurate magnetic order and phase separation in the two-dimensional Hubbard model with nearest and next-nearest neighbor hopping, *Phys. Rev. B* **81**, 094407 (2010).
 - [2] P. B. Visscher, Phase separation instability in the Hubbard model, *Phys. Rev. B* **10**, 943 (1973).
 - [3] P.A. Igoshev, M.A. Timirgazin, V.F. Gilmutdinov, A.K. Arzhnikov and V.Yu. Irkhin, Spiral magnetism in the single-band Hubbard model: the Hartree-Fock and slave-boson approaches, *J. Phys.: Condens. Matter* **27**, 446002 (2015).
 - [4] V. Yu. Irkhin, Yu. P. Irkhin. Many-electron operator approach in the solid state theory, *phys. stat. sol. (b)* **183**, 9 (1994).
 - [5] P. W. Anderson. Theories of high-temperature superconductivity, *Int. J. Mod. Phys. B* **4**, 181 (1990).
 - [6] C. L. Kane, P. A. Lee, N. Read, Motion of a single hole in a quantum antiferromagnet. *Phys. Rev. B* **39**, 6880 (1989).
 - [7] G. Kotliar and A. E. Ruckenstein, New Functional Integral Approach to Strongly Correlated Fermi Systems: The Gutzwiller Approximation as a Saddle Point, *Phys. Rev. Lett.* **57**, 1362 (1986).
 - [8] V. Yu. Irkhin, M. I. Katsnelson, Ground state and electron-magnon interaction in an itinerant ferromagnet: half-metallic ferromagnets, *J. Phys.: Condens. Matter* **2**, 7151 (1990).
 - [9] S. Florens and A. Georges, Slave-rotor mean-field theories of strongly correlated systems and the Mott transition in finite dimensions, *Phys. Rev. B* **70**, 035114 (2004).
 - [10] C. Castellani, G. Kotliar, R. Raimondi, M. Grilli, Z. Wang, and M. Rozenberg, Collective excitations, photoemission spectra, and optical gaps in strongly correlated Fermi systems, *Phys. Rev. Lett.* **69**, 2009 (1992).
 - [11] R. Fresard and P. Wölfle, Unified Slave Boson Representation of Spin and Charge Degrees of Freedom for Strongly Correlated Fermi Systems, *Int.J. Mod. Phys. B* **6**, 685 (1992).
 - [12] M. Punk and S. Sachdev, Fermi surface reconstruction in hole-doped t-J models without long-range antiferromagnetic order, *Phys. Rev. B* **85**, 195123 (2012).
 - [13] T. C. Ribeiro and X.-G. Wen, Doped carrier formulation and mean-field theory of the t-t'-t"-J model, *Phys.Rev. B* **74**, 155113 (2006).
 - [14] V. Yu. Irkhin and Yu. N. Skryabin, Formation of exotic states in the s-d exchange and t-J models, *JETP Lett.* **106**, 167 (2017).
 - [15] C. Pepin, M. Lavagna, Supersymmetric Approach to Heavy-Fermion Systems, *Z. Phys.B* **103**, 259 (1997).
 - [16] M. A. Timirgazin, P. A. Igoshev, A. K. Arzhnikov, V. Yu. Irkhin, Metal-Insulator Transition in the Hubbard Model: Correlations and Spiral Magnetic Structures, *J. Low Temp. Phys.* **185**, 651 (2016).
 - [17] M. A. Timirgazin, P. A. Igoshev, A. K. Arzhnikov, V. Yu. Irkhin, Magnetic States, Correlation Effects and Metal-Insulator Transition in FCC Lattice, *J. Phys.: Condens. Matter* **28**, 505601 (2016).
 - [18] P.A. Igoshev, M.A. Timirgazin, A.K. Arzhnikov, T.V. Antipin, V.Yu. Irkhin, Spiral magnetic order, non-uniform states and electron correlations in the conducting transition metal systems, *J. Magn. Magn. Mater.* **440**, 66 (2017).
 - [19] M. I. Auslender, V. Yu. Irkhin, M. I. Katsnelson, Itinerant electron ferromagnetism in narrow energy bands, *J. Phys. C: Solid State Phys.* **21**, 5521 (1988).